ELSEVIER

International Journal of Solids and Structures 41 (2004) 5499–5515

INTERNATIONAL JOURNAL OF SOLIDS and STRUCTURES

www.elsevier.com/locate/ijsolstr

A fracture mechanics model for a composite beam with multiple reinforcements under cyclic bending

Andrea Carpinteri *, Andrea Spagnoli, Sabrina Vantadori

Department of Civil and Environmental Engineering and Architecture, University of Parma, Parco Area delle Scienze 181/A, 43100 Parma, Italy

Received 15 April 2004; received in revised form 15 April 2004
Available online 2 June 2004

Abstract

The flexural behaviour of a composite beam (e.g. a reinforced concrete beam) with multiple reinforcements under cyclic loading is analysed through a fracture mechanics-based theoretical model which considers a cracked beam subjected to an external bending moment and the crack bridging reactions due to the reinforcements. Assuming a rigid-perfectly plastic bridging law for the reinforcements and a linear-elastic law for the matrix, the statically indeterminate bridging forces are obtained from compatibility conditions. Typical phenomena, such as elastic shake-down and plastic shake-down, in the composite beam under cyclic bending are described in terms of applied bending moment against beam cross-section rotation. Further, by employing a fatigue crack growth law (e.g. the Paris law), the mechanical behaviour of the examined beam up to failure can be captured. Some numerical examples to illustrate the capabilities of the proposed theoretical model are presented.

Keywords: Bridged crack; Crack growth; Fatigue; Brittle-matrix composite; Shake-down

1. Introduction

Many composite materials used in different engineering applications consist of a brittle matrix and ductile reinforcements (e.g. bars, wires, fibers). By incorporating such reinforcements into the matrix, several mechanical properties are enhanced, including: cracking resistance, ductility, impact resistance, fatigue strength. In the field of civil engineering, for instance, fiber-reinforced cementitious composites are employed in an increasing amount of structures (e.g. airport pavements, highway overlays, bridge decks, machine foundations, shear walls) which are subjected to repeated loadings during their service life. Such loadings are characterized by a number of cycles ranging from few hundreds (as for shear walls under seismic loading) to hundreds of millions (as for foundations supporting dynamic machines).

* Corresponding author. Tel.: +39-0521-905922; fax: +39-0521-905924.
E-mail address: andrea.carpinteri@unipr.it (A. Carpinteri).

0020-7683/$ - see front matter © 2004 Elsevier Ltd. All rights reserved.
doi:10.1016/j.ijsolstr.2004.04.032

Nomenclature

a	crack depth
b	height of the beam cross-section
c_i	position of the ith reinforcement with respect to the bottom of the beam cross-section
E	Young modulus of the matrix
f_c	compressive strength of the matrix
F_i	bridging force (reaction) of the ith reinforcement
$F_{P,i}$	ultimate force (reaction) of the ith reinforcement
K_I	stress intensity factor
K_{IC}	critical stress intensity factor (fracture toughness)
M	bending moment
M_F	bending moment of either unstable fracture or crushing of the matrix
M_{max}	maximum bending moment
M_{min}	minimum bending moment
M_P	plastic bending moment
M_{SD}	shake-down bending moment
n	number of reinforcements intersected by the crack
N	number of loading cycles
N_f	number of loading cycles to failure
N_P	brittleness number
t	thickness of the beam cross-section
w_i	crack opening translation at the ith reinforcement level
$\beta^{(k)}$	load factor related to the load step k
$\zeta_i = c_i/b$	relative position of the ith reinforcement with respect to the bottom of the beam cross-section
λ_{ij}	localised compliance related to the crack opening translation at the ith reinforcement level due to a unit crack opening force $F_j = 1$ acting at ζ_j
λ_{iM}	localised compliance related to the crack opening translation at the ith reinforcement level due to a unit bending moment $M = 1$
λ_{MM}	rotational localised compliance due to a unit bending moment $M = 1$
$\xi = a/b$	relative crack depth
σ_c	compressive stress in the matrix
φ	rotation of the cracked beam cross-section

Subscripts

0	referring to the preceding load reversal
i	referring to the ith reinforcement intersected by the crack, with $i = 1, \ldots, n$
j	referring to the jth reinforcement intersected by the crack, with $j = 1, \ldots, n$

Superscripts

~	referring to a dimensionless (normalised) parameter
(k)	referring to the load step k
(N)	referring to the Nth loading cycle, with $N = 1, \ldots, N_f$

Other symbols are defined as they appear in the text.

Cracks might develop in structures of reinforced brittle-matrix composite materials, so that the overall mechanical behaviour would strongly be affected by the crack bridging reactions of the reinforcements. Moreover, the progressive crack growth under cyclic loading influences the bridging behaviour, and causes significant changes in the mechanical properties of the above materials (strength, toughness, stiffness, hysteretic behaviour, etc.), eventually leading to failure. A number of theoretical models have been proposed to describe such phenomena and to predict fatigue life (for instance, see recent models for fiber-reinforced concrete structural components subjected to cyclic bending, discussed in Zhang and Stang (1998), Zhang et al. (1999) and Matsumoto and Li (1999)).

In the present paper, a fracture mechanics-based model is proposed to analyse the flexural behaviour of a composite beam with multiple reinforcements under cyclic loading. Such a model considers a cracked portion of a beam subjected to an external bending moment and the crack bridging reactions due to the reinforcements (Fig. 1). Assuming a rigid-perfectly plastic bridging law for the reinforcements and a linear-elastic law for the matrix, the statically indeterminate bridging forces are obtained from compatibility conditions related to the crack opening translations at the levels of the reinforcements. Typical phenomena, such as elastic shake-down and plastic shake-down, are described in terms of applied bending moment against beam cross-section rotation. Finally, the flexural behaviour of the composite beam up to failure is captured by applying the well-known Paris fatigue crack growth law, and some numerical examples to illustrate the capabilities of the present theoretical model are discussed.

The model here proposed originates from previous formulations for monotonic loading applied to beams with either a single reinforcement (Carpinteri Al, 1984) or multiple reinforcements (Carpinteri Al and Massabò, 1996, 1997), while only the cases of either a single reinforcement (Carpinteri Al and Carpinteri An, 1984; Carpinteri An, 1991; Carpinteri An, 1992) or two reinforcements (Carpinteri Al and Puzzi, 2003) have so far been analysed for cyclic loading. Note that, in the aforementioned works, the compatibility conditions considered for determining the statically indeterminate reinforcement reactions

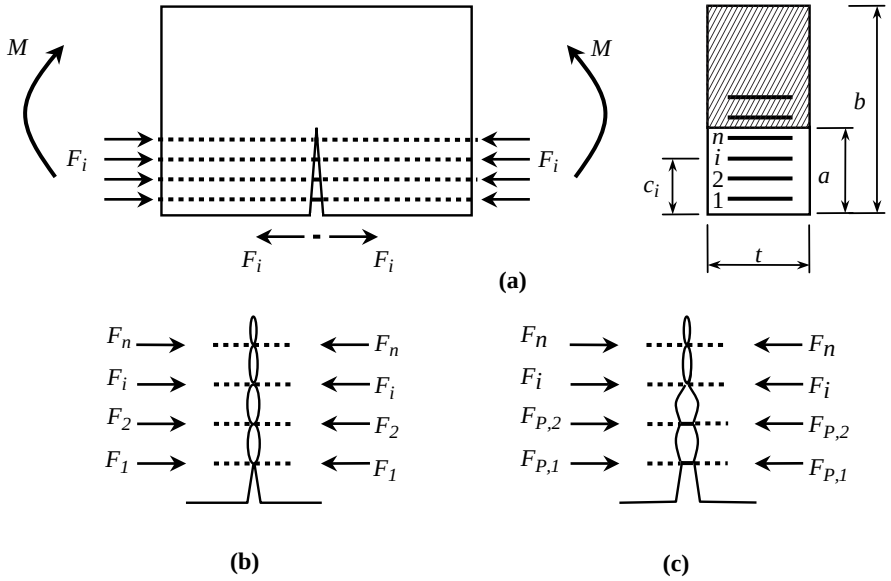

Fig. 1. (a) Schematic of the model; (b) crack profile for elastic reinforcements; (c) crack profile for yielded or slipped reinforcements.

are related to the rotation of the cracked beam cross-section in the case of a single reinforcement, and to crack opening translations in the case of multiple reinforcements.

2. Description of the model

2.1. Model assumptions

The model considers a cracked portion of a composite beam with a rectangular cross-section under bending M (Fig. 1). The crack is assumed to be subjected to Mode I loading (i.e. the crack is normal to the longitudinal axis of the beam). Reinforcements are discretely distributed across the crack and oriented along the longitudinal axis of the beam. Although the problem being considered is three-dimensional in nature, it is herein approximately treated as a two-dimensional one.

The height and thickness of the beam cross-section are equal to b and t, respectively, whereas the crack depth is called a (Fig. 1(a)). The position of the ith reinforcement ($i = 1, \ldots, n$, where n is the number of reinforcements intersected by the crack) is described by the distance c_i with respect to the bottom of the beam cross-section. Note that the reinforcement numbers are sorted according to the reinforcement positions along the beam height, by assuming that reinforcement No. 1 is the nearest to the bottom of the beam cross-section. The relative crack depth $\xi = a/b$ and the normalised coordinate $\zeta_i = c_i/b$ are also defined.

The mechanical behaviour of the composite beam is as follows. The matrix (treated as a homogeneous and isotropic material) is assumed to present a linear elastic constitutive law, whereas the reinforcements are assumed to behave as rigid-perfectly plastic (symmetric in both tension and compression) bridging elements which connect together the two surfaces of the crack. Such a behaviour originates from an approximating relationship between the bridging force carried by a single reinforcement (understood as a pullout force for the reinforcement) and the related translation of the reinforcement in correspondence to the crack surface, assuming that the translation is solely due to the slip at the reinforcement–matrix interface under constant frictional bond when the debonding zone has fully developed (i.e. when the length of the slip activated zone equates either the length of the reinforcement embedded into the matrix or its anchorage length). The above fully debonded condition is hereafter termed 'slippage' of the reinforcement. Moreover, in order to account for failure of the reinforcement material itself, it is assumed that the infinitesimal uncovered reinforcement segment between the two crack surfaces can plastically flow under the bridging force (this condition is hereafter termed 'yielding' of the reinforcement) and, therefore, ignoring elastic deformation in the reinforcement, a rigid-perfectly plastic constitutive law is assumed for the reinforcement. Hence, the rigid-perfectly plastic bridging law of the generic (ith) reinforcement is characterised by an ultimate force $F_{\mathrm{P},i}$ (and $-F_{\mathrm{P},i}$ in compression) corresponding to either slippage or yielding, whichever of them exhibits the minimum absolute value.

The loading process presents constant amplitude cycles of the bending moment M, ranging from $M_{\min}$ to $M_{\max}$ (Fig. 2). Note that, for negative values of $M_{\min}$, the tensile stress at the top of the beam cross-section should be lower than the tensile strength of the matrix. The successive cross-sectional configurations during the loading process must satisfy equilibrium and compatibility conditions. Since the problem being examined is statically indeterminate, the unknown reinforcement reactions F_i (with $i = 1, \ldots, n$) on the matrix can be deduced from n kinematic conditions related to the crack opening translations w_i at the different reinforcement levels, as is discussed below. If $|F_i|$ is equal to $F_{\mathrm{P},i}$, the force of the ith reinforcement becomes known, and the crack opening translations are hereafter shown to depend on such a value. According to the present model, no cycle-dependent degradation of either the interfacial bond or the yield

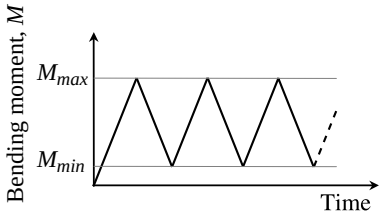

Fig. 2. Cycles of bending moment.

strength is considered and, hence, the ultimate forces $F_{P,i}$ (with $i = 1, \ldots, n$) are assumed to be constant as the number of loading cycles increases.

2.2. Monotonic loading

First of all, consider the cracked composite beam subjected to a bending moment M (opening the crack) monotonically increasing. As is mentioned above, the matrix behaves in a linear elastic manner. Therefore, linear elastic fracture mechanics can be applied, and the crack opening translation w_i at the ith reinforcement level is obtained through the superposition principle and the localised compliances due to the crack (see Appendix A):

$$w_i = w_{iM} + \sum_{j=1}^{n} w_{ij} = \lambda_{iM} M - \sum_{j=1}^{n} \lambda_{ij} F_j \tag{1}$$

where w_{iM} and w_{ij} are the crack opening translations produced by the bending moment M and by the generic reaction F_j (assumed to be positive when the jth reinforcement is under tension), respectively; the localised compliances, λ_{iM} and λ_{ij}, due to the crack represent the ith crack opening translation for $M = 1$ and that for a unit crack opening force, $F_j = 1$, acting at ζ_j, respectively.

The kinematic equations to determine the unknown reinforcement reactions can be deduced from congruence conditions. In other words, because of the rigid-perfectly plastic laws for the reinforcements and the reinforcement–matrix interface, compatibility requires that w_i ($i = 1, \ldots, n$) be equal to zero until yielding or slippage of at least one of the n reinforcements is reached (Fig. 1(b) and (c)). Using matrix formulation, this compatibility condition reads:

$$\{w\} = \{\lambda_M\} M - [\lambda]\{F\} = \{0\} \tag{2}$$

where $\{w\} = \{w_1, \ldots, w_n\}^{\mathrm{T}}$ is the vector of the crack opening translations at the different reinforcement levels, and $\{F\} = \{F_1, \ldots, F_n\}^{\mathrm{T}}$ is the vector of the unknown bridging forces. Further, $\{\lambda_M\}$ is the vector of the localised compliances related to the bending moment M, whereas $[\lambda]$ is a symmetric square matrix of order n, whose generic element ij (ith row, jth column) represents the localised compliance λ_{ij}. Hence, the unknown vector $\{F\}$ can be obtained from Eq. (2):

$$\{F\} = [\lambda]^{-1}\{\lambda_M\} M \tag{3}$$

If the generic (ith) reinforcement yields or slips, the crack opens at the coordinate ζ_i, and w_i becomes an unknown quantity. Therefore, the number of kinematic conditions in Eq. (2) reduces by one, along with the degree of statical redundancy, F_i being equal to the previously defined maximum bridging force $F_{P,i}$. Consequently, the number of equations which can be written $(n - 1)$ continues to be equal to the number of unknowns $(n - 1)$. At the subsequent yielding or slippage of some reinforcement, the number of kinematic conditions reduces further along with the number of statically indeterminate forces.

In order to account for the previously yielded or slipped reinforcements, the compatibility condition of Eq. (2) can formally be written as follows:

$$\{w\} = [H]\left(\{\lambda_M\}M - [\lambda]\left\{\overline{F}\right\}\right) = \{0\} \tag{4}$$

where $[H]$ is a diagonal matrix whose generic element ii is given by the Heaviside function $H(x)$ with $x = 1 - |F_i|/F_{\mathrm{P},i}$ ($H(x) = 1$ for $x > 0$, $H(x) = 0$ for $x \leqslant 0$), and

$$\left\{\overline{F}\right\} = [H]\{F\} + ([I] - [H])\{F_\mathrm{P}\} \tag{5}$$

with $\{F_\mathrm{P}\} = \{F_{\mathrm{P},1}, \ldots, F_{\mathrm{P},n}\}^\mathrm{T}$, whereas $[I]$ is the unit matrix of order n. Note that, since the matrix $[H]$ becomes singular when at least one reinforcement yields or slips, equation(s) related to $H_{ii} = 0$ must be eliminated for solving Eq. (4). Moreover, it should be remarked that, being the matrix $[H]$ a function of the solution vector $\{F\}$, an iterative procedure is in principle required to solve Eq. (4), but another method is proposed in the following.

After determining the solution vector $\{F\}$ from Eq. (4), the vector $\left\{\overline{F}\right\}$ is obtained from Eq. (5), and the crack opening translations $\{w\}$ are computed as follows:

$$\{w\} = \{\lambda_M\}M - [\lambda]\left\{\overline{F}\right\} \tag{6}$$

The relative rotation φ due to the crack only (i.e. excluding the elastic deformation of the matrix) of the two extreme cross-sections of the beam portion in Fig. 1(a) is given by:

$$\varphi = \lambda_{MM}M - \{\lambda_M\}^\mathrm{T}\left\{\overline{F}\right\} \tag{7}$$

where λ_{MM} is reported in Eq. (A.13). Eq. (7) is deduced by applying the Castigliano theorem, namely, $\varphi = \partial U/\partial M = -\partial W/\partial M$, where U and W are the variations of, respectively, the strain energy and the total potential energy of the body due to the introduction of the crack, with the applied loads (external bending moment and reinforcement reactions) kept constant. The variation W of the total potential energy can be computed by substituting the expressions (A.7) and (A.8) in Eq. (A.5).

Note that the collapse of the beam under the applied bending moment might occur because of two possible reasons: (1) unstable fracture of the matrix (when the toughness K_{IC} of the material is attained, that is, $K_I = K_{IC}$, where the stress intensity factor K_I is obtained through the superposition principle: $K_I = K_{IM} - \sum_{i=1}^{n} K_{Ii}$, with K_{IM} and K_{Ii} given by Eqs. (A.7) and (A.8), respectively), or (2) crushing of the matrix (when the normal compressive stress σ_c, computed through the classical bending theory applied to the ligament, attains the material strength f_c).

2.3. Cyclic loading

Reinforcements under cyclic bending moment might undergo plastic-to-rigid transitions at load reversals. Hence, the compatibility condition of Eq. (4) is modified in order to consider possible non-zero translations $\{w\}$ at reversals:

$$\{w\} - \{w_0\} = [H]\left(\{\lambda_M\}(M - M_0) - [\lambda]\left(\left\{\overline{F}\right\} - \left\{\overline{F}_0\right\}\right)\right) = \{0\} \tag{8}$$

with $\left\{\overline{F}\right\}$ given by:

$$\left\{\overline{F}\right\} = [H]\{F\} + q([I] - [H])\{F_\mathrm{P}\} \tag{9}$$

where $q = 1$ during loading and $q = -1$ during unloading. The subscript '0' refers to the values of some parameters (crack opening translations, bending moment and reinforcement reactions) at the preceding load reversal. Obviously, the quantities related to the subscript '0' are equal to zero at the beginning of the

loading process, i.e. at the first loading half-cycle. Once the solution vector $\{F\}$ is obtained from Eq. (8), $\{\overline{F}\}$ can be computed by Eq. (9), and crack displacements can be deduced by Eqs. (6) and (7).

The crack is herein assumed to propagate (under cyclic loading) according to the Paris law ($\mathrm{d}a/\mathrm{d}N = C\Delta K_I^m$; Paris and Erdogan, 1963). For convenience, increments of crack length due to fatigue crack growth are determined after every block of a given number of cycles. Note that the above increments imply an increase of localised compliances at constant applied loads (i.e. bending moment M and bridging forces $\{F\}$).

2.4. Model implementation

The calculation procedure for the theoretical model here presented is as follows:

1. Compute the localised compliances (see Eqs. (A.11)–(A.13)) for the beam being considered, with a given value of the initial crack length ξ_{init}.
2. At the generic load step k, determine the solution vector $\{F^{(k)}\}$ from Eq. (8), by posing either $M = M_{\max}$ (during loading) or $M = M_{\min}$ (during unloading). Calculate the load factor $\beta^{(k)}$ for which the most highly stressed reinforcement is on the verge of its yielding or slippage:
$$\beta^{(k)} = \max_{1 \leqslant i \leqslant n} \left\{ \frac{F_i^{(k)} - F_i^{(k-1)}}{qF_{\mathrm{P},i} - F_i^{(k-1)}} \right\} \tag{10}$$
where $q = 1$ during loading and $q = -1$ during unloading. Note that, when the $\beta^{(k)}$ value computed from Eq. (10) results to be lower than 1 (that occurs when no reinforcement yields or slips during an unloading and/or loading half-cycle), the load factor is posed as equal to the unity (see Eqs. (11) and (12) to better understand such a position).
3. From the load factor $\beta^{(k)}$, calculate the moment $M^{(k)}$ for which the most highly stressed reinforcement is on the verge of its yielding or slippage, namely:
$$M^{(k)} = \frac{M - M^{(k-1)}}{\beta^{(k)}} + M^{(k-1)} \tag{11}$$
where $M = M_{\max}$ during loading and $M = M_{\min}$ during unloading.
Note that, at a load step k corresponding to either a loading–unloading reversal or an unloading–reloading reversal, $\beta^{(k)}$ is equal to 1 and, according to Eq. (11), $M^{(k)}$ results to be equal to either $M_{\max}$ or $M_{\min}$. Further, at the first load step k after a loading–unloading reversal, $M^{(k-1)}$ is equal to $M_{\max}$ whereas, at the first load step k after an unloading–reloading reversal, $M^{(k-1)}$ is equal to $M_{\min}$. Then, it can be remarked that, at the very first load step (i.e. $k = 1$), $M^{(k-1)} = M^{(0)}$ is equal to 0.
4. Update the reinforcement reactions:
$$\{F^{(k)}\} = \frac{\{F^{(k)}\} - \{F^{(k-1)}\}}{\beta^{(k)}} + \{F^{(k-1)}\} \tag{12}$$
5. Calculate the rotation $\varphi^{(k)}$ according to Eq. (7), by substituting M with $M^{(k)}$ (determined from Eq. (11)) and $\{\overline{F}\}$ with $\{\overline{F}^{(k)}\}$, where $\{\overline{F}^{(k)}\}$ is obtained from Eqs. (9) and (12).
6. If the load step k terminates at a reversal, store the crack opening translations $\{w^{(k)}\}$ $\left(\text{computed through Eq. (6), with } M = M^{(k)} \text{ and } \{\overline{F}\} = \{\overline{F}^{(k)}\}\right)$.
7. Stop if $K_I = K_{IC}$ or if the compressive strength f_c is attained in the matrix.
8. Increase the crack length according to the Paris law and update the localised compliances.
9. Return to step No. 2 of the present procedure.

3. Bending moment vs rotation response

3.1. Shake-down behaviour

The proposed theoretical model can be illustrated by applying it to some simple cases which point out all its essential features. The overall response of the cracked beam cross-section under cyclic bending is qualitatively analysed in terms of applied bending moment vs cross-section rotation curves.

Firstly, the case of a single reinforcement is considered. Under certain values of loading and mechanical and geometrical parameters, the bending moment vs rotation curve for a single cycle might look like that reported in Fig. 3. The numbers (from 1 to 6) in the graph indicate the sequence of the load steps, while the upwards and downwards triangular symbols refer to tensile and compressive yielding/slippage of the reinforcement, respectively. It can be noted that the most significant values of the bending moment in a loading cycle are: the plastic bending moment M_P (equal to $M^{(1)}$) which produces yielding or slippage in the reinforcement (subjected to tension) during loading, and the shake-down bending moment M_{SD} (equal to $M^{(5)}$) above which yielding or slippage in the reinforcement (subjected to compression) occurs during unloading (see load step No. 3, represented by the segment 2–3 in Fig. 3).

With reference to the above case, the following regions of behaviour can be observed:

(i) elastic behaviour for $0 \leqslant M_{max} < M_P$;
(ii) elastic shake-down for $M_P \leqslant M_{max} < M_{SD}$;
(iii) plastic shake-down for $M_{SD} \leqslant M_{max} < M_F$ ($M_F =$ bending moment of matrix unstable fracture when K_I attains K_{IC}, or bending moment of matrix crushing when the compressive strength f_c is attained).

Note that, in the case of plastic shake-down, the bending moment vs rotation curve describes a hysteretic loop (for the example displayed in Fig. 3, the energy dissipated in each cycle is equal to the area 2–3–4–5–6).

Now let us consider a beam with multiple reinforcements. For the sake of simplicity, three identical reinforcements are assumed, and the bending moment against rotation curve is shown in Fig. 4. As in the previous case, the numbers in the graph indicate the sequence of the load steps, while the upwards and downwards triangular symbols refer to tensile and compressive yielding/slippage of the reinforcements, respectively. The plastic bending moment M_P (equal to $M^{(1)}$) and the shake-down bending moment M_{SD} (equal to $M^{(9)}$) are displayed, and the aforementioned three regions of behaviour can be observed. The energy dissipated in each cycle is equal to the area of the hysteretic loop 4–5–6–7–8–9–10–11–12.

Some further observations can be made for the case being examined. Each reinforcement is characterised by a plastic bending moment $M_{P,i}$ and a shake-down bending moment $M_{SD,i}$: $M_{P,1}$, $M_{P,2}$ and $M_{P,3}$ correspond

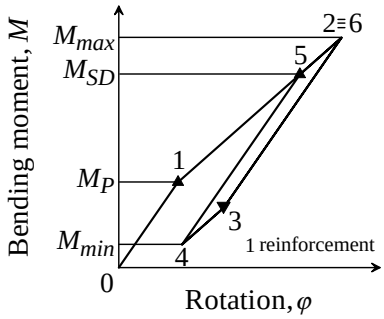

Fig. 3. Typical bending moment vs rotation hysteretic loop in the case of a single reinforcement.

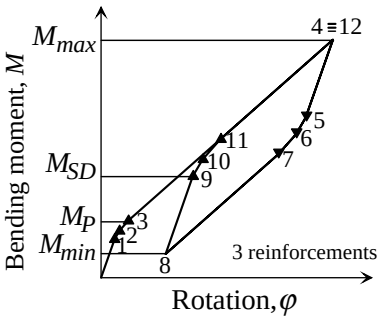

Fig. 4. Typical bending moment vs rotation hysteretic loop in the case of three reinforcements.

to $M^{(1)}$, $M^{(2)}$ and $M^{(3)}$, respectively, whereas $M_{SD,1}$, $M_{SD,2}$ and $M_{SD,3}$ correspond to $M^{(9)}$, $M^{(10)}$ and $M^{(11)}$, respectively (Fig. 4). Obviously, the overall plastic bending moment M_P, defining the transition from elastic behaviour to elastic shake-down, is given by the minimum among the reinforcement plastic bending moments $M_{P,i}$, as well as the overall shake-down bending moment M_{SD}, defining the transition from elastic shake-down to plastic shake-down, is given by the minimum among the reinforcement shake-down bending moments $M_{SD,i}$. Intermediate regions of behaviour, where only certain reinforcements undergo yielding/slippage in tension and/or compression, can be conceived: for instance, if we had $M_{SD,2} < M_{max} < M_{SD,3}$, tensile yielding or slippage in the three reinforcements and compressive yielding or slippage in only two reinforcements would occur.

The observations made for the cases in Figs. 3 and 4 can be extended to the general case of n reinforcements. Hence, the following general relationships can be written:

$$M_{P,i} = M^{(k)} \tag{13}$$

where k refers to the load step for which the ith reinforcement is on the verge of its yielding or slippage in tension, and

$$M_{SD,i} = M_{max} - M^{(k)} + M_{min} \tag{14}$$

where k now refers to the load step for which the ith reinforcement is on the verge of its yielding or slippage in compression. Then the overall plastic and shake-down bending moments are given by:

$$M_P = \min\{M_{P,i}\} \tag{15a}$$

$$M_{SD} = \min\{M_{SD,i}\} \tag{15b}$$

It should be noted that the following relationship between $M_{P,i}$ and $M_{SD,i}$ of the generic (ith) reinforcement holds:

$$M_{SD,i} = 2M_{P,i} + M_{min} \tag{16}$$

In the region of plastic shake-down behaviour ($M_{SD} \leqslant M_{max} < M_F$), the energy dissipated per cycle can be calculated as follows:

$$\frac{\text{work}}{\text{cycle}} = \sum_{k=s_b}^{s_e} \frac{1}{2}\left(M^{(k+1)} + M^{(k)}\right)\left(\varphi^{(k+1)} - \varphi^{(k)}\right) \tag{17}$$

where s_b = load step at the beginning of the cycle, and s_e = load step at the end of the cycle (e.g. $s_b = 4$ and $s_e = 12$ for the cycle in Fig. 4).

It might be worth pointing out that, by employing the proposed model and assuming a non-propagating crack in the composite beam being considered, the cyclic flexural behaviour described above in terms of bending moment against beam cross-section rotation is reminiscent of that predicted through a classical constitutive theory for cyclic plasticity with a linear-piecewise kinematic hardening rule (e.g. see Chaboche, 1986, for a review, and Masing, 1926, for his early parallel sub-element model). As a consequence, no ratchetting effect (accumulated plastic deformations) can be accounted for by the present model.

According to the dimensional analysis and within the range of validity of the model assumptions (see Carpinteri Al and Massabò, 1997, for monotonic loading), the bending moment vs rotation relationship, M vs φ (see Eq. (7)), can be written in the following dimensionless form provided that the geometrical parameters t/b, ξ and ζ_i $(i = 1, \ldots, n)$ are fixed, the ultimate forces $F_{\mathrm{P},i}$ $(i = 1, \ldots, n)$ are identical to one another and failure is supposed to be caused by unstable fracture of the matrix:

$$\widetilde{M} = f\left(\varphi, N_{\mathrm{P}}, \widetilde{E}\right) \tag{18}$$

where

$$\widetilde{M} = \frac{M}{K_{IC} b^{2.5}} \tag{19a}$$

$$N_{\mathrm{P}} = \frac{\sum_{i=1}^{n} F_{Pi}}{K_{IC} b^{0.5} t} \tag{19b}$$

$$\widetilde{E} = \frac{E b^{0.5}}{K_{IC}} \tag{19c}$$

Moreover, in the last paper mentioned above, it has been shown that the dimensionless bending moment vs normalised rotation relationship, $\widetilde{M}$ vs $\tilde{\varphi}$ (with $\tilde{\varphi} = \varphi \widetilde{E}$), is solely controlled by the dimensionless parameter N_{P} (called brittleness number after Carpinteri Al, 1984), namely, the cyclic flexural responses of beams having different values of the mechanical and geometrical parameters are physically similar to one another if the number N_{P} is the same.

3.2. Fatigue crack growth

Now let us consider the crack propagation according to the Paris law. The case of three identical reinforcements, analogous to the case in Fig. 4, is examined. Fig. 5 shows bending moment vs rotation curves at different numbers of loading cycles (the first cycle, the generic Nth cycle, and the final N_fth cycle). It can be remarked that, as the crack propagates, the values of the local compliances (see Eqs. (A.11)–(A.13)) increase and, hence, the slopes of the linear segments in the diagram M vs φ decrease. Further, by increasing ξ, the value of the shake-down bending moment M_{SD} (see $M_{\mathrm{SD}}^{(1)}$, $M_{\mathrm{SD}}^{(N)}$ and $M_{\mathrm{SD}}^{(N_f)}$ in Fig. 5) decreases. Consequently, the energy dissipated at every hysteretic loop varies as the number of loading cycles increases. Finally, the fatigue collapse of the beam can occur due to either matrix unstable fracture, when K_I attains K_{IC}, or matrix crushing, when σ_{c} attains f_{c}.

4. Numerical examples

Consider a reinforced concrete beam cross-section with $t = 0.2$ m, $b = 0.3$ m, submitted to pulsating cyclic bending ($M_{\min} = 0$). The concrete mechanical properties E and K_{IC} are assumed to be equal to 32.1 GPa and 1.75 MPa $\sqrt{\mathrm{m}}$, respectively. Further, in the present section, the concrete compressive strength is

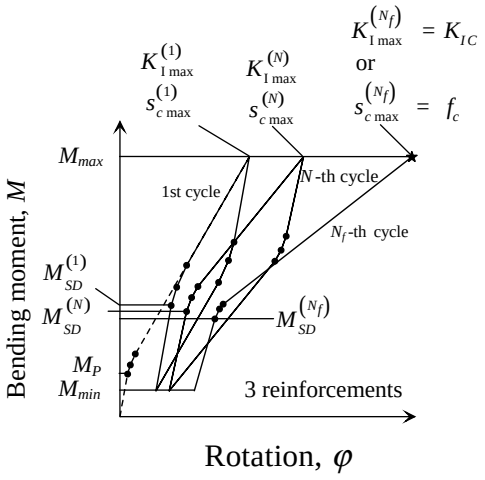

Fig. 5. Typical bending moment vs rotation hysteretic loops at different numbers of loading cycles, in the case of three reinforcements.

assumed to be as high as to avoid crushing failure (that is, failure is supposed to be caused by unstable fracture of the matrix in the following examples).

Firstly, let us examine the case of a single reinforcement at $\zeta_1 = 0.1$, with an ultimate force equal to 10,053 N (e.g. corresponding to a steel bar of diameter 8 mm and yield strength equal to 200 MPa), so that the brittleness number N_P is equal to about 0.05. By varying, for instance, the reinforcement percentage, different values of N_P could be obtained: three possible values, considered in the following examples, are 0.02, 0.05 and 0.10.

Fig. 6 shows the variation of the dimensionless (see Eq. (19a)) shake-down ($\widetilde{M}_{SD}$, with $\widetilde{M}_{SD} = 2\widetilde{M}_P$ for $\widetilde{M}_{min} = 0$, see Eq. (16)) and unstable fracture ($\widetilde{M}_F$) bending moments against the relative crack depth ξ, for the three above values of N_P. It can be remarked that both such characteristic bending moments decrease

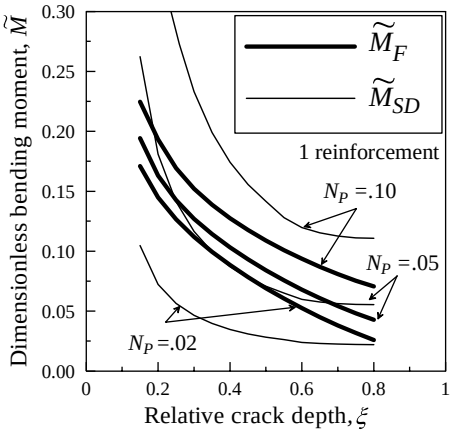

Fig. 6. Dimensionless shake-down $\left(\widetilde{M}_{SD}\right)$ and unstable fracture $\left(\widetilde{M}_F\right)$ bending moments vs relative crack depth, for $\widetilde{M}_{min} = 0$ and a single-reinforcement beam with different values of the brittleness number N_P.

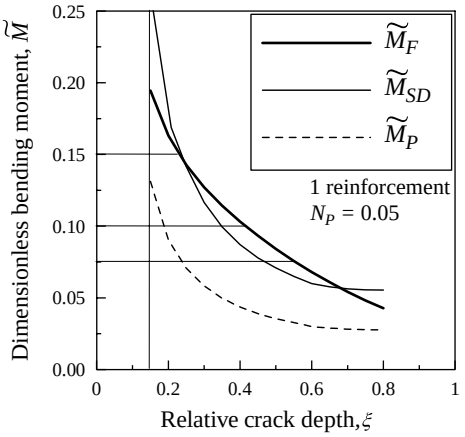

Fig. 7. Dimensionless plastic $\left(\widetilde{M}_{\mathrm{P}}\right)$, shake-down $\left(\widetilde{M}_{\mathrm{SD}}\right)$ and unstable fracture $\left(\widetilde{M}_{\mathrm{F}}\right)$ bending moments vs relative crack depth, for $\widetilde{M}_{\min} = 0$ and a single-reinforcement beam with $N_{\mathrm{P}} = 0.05$.

with increasing ξ but, depending on the values of ξ and N_{P}, $\widetilde{M}_{\mathrm{F}}$ can be higher or lower than $\widetilde{M}_{\mathrm{SD}}$. Clearly, unstable fracture tends to precede elastic and/or plastic shake-down as the brittleness number N_{P} increases.

By selecting a dimensionless maximum bending moment $\widetilde{M}_{\max}$ and an initial relative crack depth ξ_{init}, the three regions of behaviour previously described (elastic behaviour, elastic shake-down and plastic shake-down) can be encountered as the crack undertakes fatigue propagation (i.e. ξ increases). For instance, by assuming $\widetilde{M}_{\max} = 0.075$, $\xi_{\mathrm{init}} = 0.15$ and $N_{\mathrm{P}} = 0.05$ (Fig. 7), we encounter an elastic behaviour for $0.15 \leqslant \xi < 0.24$, an elastic shake-down for $0.24 \leqslant \xi < 0.47$, and a plastic shake-down for $0.47 \leqslant \xi$ up to unstable fracture failure at $\xi = 0.55$.

Taking advantage of Fig. 7, two significant loading cases ($\widetilde{M}_{\max}$ equal to 0.10 and 0.15, respectively) are considered for the cracked beam with $N_{\mathrm{P}} = 0.05$ and $\xi_{\mathrm{init}} = 0.15$. Assuming typical values of the Paris law parameters for plain concrete ($C = 7.71 \times 10^{-25}$ and $m = 3.12$ for crack growth rate and stress–intensity range expressed in m/cycle and $\mathrm{Nm}^{-3/2}$, respectively; Baluch et al., 1987), dimensionless bending moment $\widetilde{M}$ against normalised rotation $\tilde{\varphi}$ (with $\tilde{\varphi} = \varphi\widetilde{E}$, and $\widetilde{E}$ given by Eq. (19c)) cyclic curves up to fatigue failure can be determined through the proposed theoretical model (Fig. 8). Crack propagation has been calculated every 100 loading cycles for computational efficiency, whereas the results in Figs. 8 and 9 are plotted for some numbers of loading cycles only. It can be observed that, for $\widetilde{M}_{\max} = 0.15$ (Fig. 8(a)), the crack propagates in the elastic shake-down region (without energy dissipation in hysteretic loops) up to unstable fracture after $N_f = 2.8 \times 10^3$ cycles (see star symbol, which corresponds to $\xi = 0.23$ as also obtained from Fig. 7). On the other hand, for $\widetilde{M}_{\max} = 0.10$ (Fig. 8(b)), a transition from elastic shake-down to plastic shake-down occurs, with energy dissipation in hysteretic loops up to unstable fracture after $N_f = 23.8 \times 10^3$ cycles (see star star symbol, which corresponds to $\xi = 0.42$ as also obtained from Fig. 7).

Now consider the case of three identical reinforcements located at ζ_1, ζ_2 and ζ_3 equal to 0.06, 0.10 and 0.14, respectively, so that their centroid is at $\zeta = 0.10$ (i.e. at the same level of the single reinforcement examined above). Let us assume that $\widetilde{M}_{\max}$ be equal to 0.10, and the geometrical and mechanical parameters chosen yield $N_{\mathrm{P}} = 0.05$. Fig. 9 shows dimensionless bending moment vs normalised rotation cyclic curves up to fatigue failure after $N_f = 62.5 \times 10^3$ cycles (see star symbol, which corresponds to $\xi = 0.42$). Juxtaposing Figs. 8(b) and 9, it can be noted that, although failure occurs at the same relative crack depth ($\xi = 0.42$) in both cases, the presence of multiple reinforcements causes plastic shake-down from the very beginning of the crack growth process, while such a region of behaviour is preceded by a remarkably large

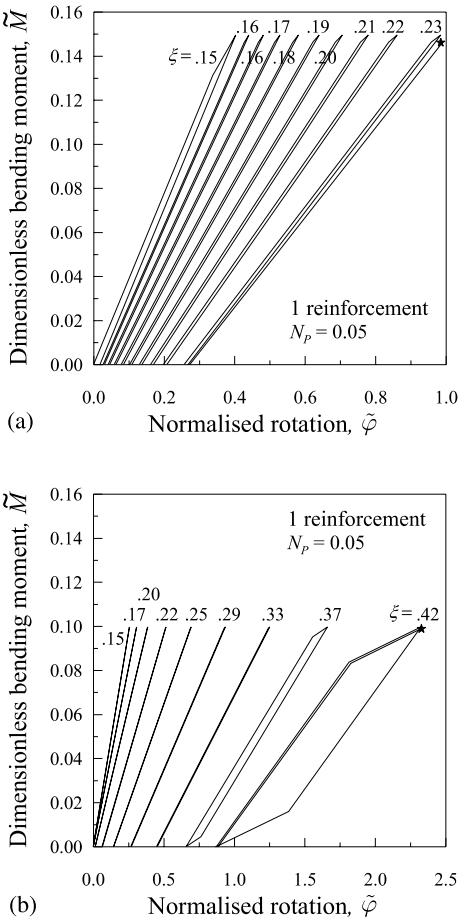

Fig. 8. Dimensionless bending moment vs normalised rotation curves, for $\tilde{M}_{\min} = 0$ and a single-reinforcement beam with $N_P = 0.05$ [the numbers near the peaks of the cyclic curves indicate the relative crack depth (ξ)]: (a) $\tilde{M}_{\max} = 0.15$, curves plotted at the first cycle ($N = 1$), after every 300 cycles and at the final cycle ($N_f = 2.8 \times 10^3$); (b) $\tilde{M}_{\max} = 0.10$, curves plotted at the first cycle ($N = 1$), after every 3000 cycles and at the final cycle ($N_f = 23.8 \times 10^3$).

zone of elastic shake-down in the case of a single reinforcement, the values of the other parameters being equal to those of the previous case. In addition, the fatigue life of the three-reinforcement beam is greater (by a factor equal to about three) than that of the single-reinforcement beam.

To summarise, the comparison between the case of a single reinforcement and that of three reinforcements ($N_P = 0.05$ for both cases) is shown in Fig. 10 in terms of the dimensionless dissipated energy (dissipated energy multiplied by $E/(K_{IC}b)^2$) per hysteretic loop against the number of loading cycles. The early stage of elastic shake-down (N less than about 20,000 loading cycles), where dissipated energy is null, can be recognised for the case of a single reinforcement. Further, it can be remarked that the total dimensionless dissipated energy computed for a single reinforcement and for three reinforcements is respectively equal to about 49 and 492. Therefore, according to the present model, by distributing the same area of reinforcement among a multiple number of elements (three elements in the example being considered), the energy dissipation capacity of the beam as well as its fatigue life (see also the final part of the previous paragraph) significantly increase.

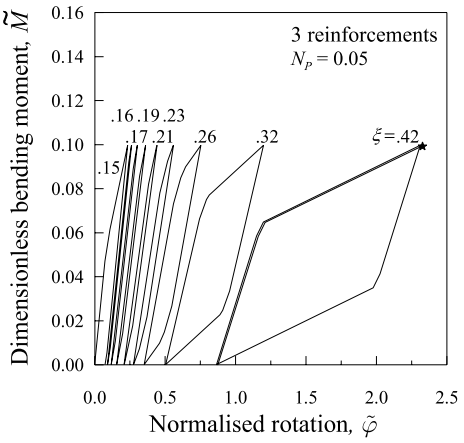

Fig. 9. Dimensionless bending moment vs normalised rotation curves, for $\widetilde{M}_{\min} = 0$, $\widetilde{M}_{\max} = 0.10$ and a three-reinforcement beam with $N_{\mathrm{P}} = 0.05$, plotted at the first cycle ($N = 1$), after every 8000 cycles and at the final cycle ($N_f = 62.5 \times 10^3$) [the numbers near the peaks of the cyclic curves indicate the relative crack depth (ξ)].

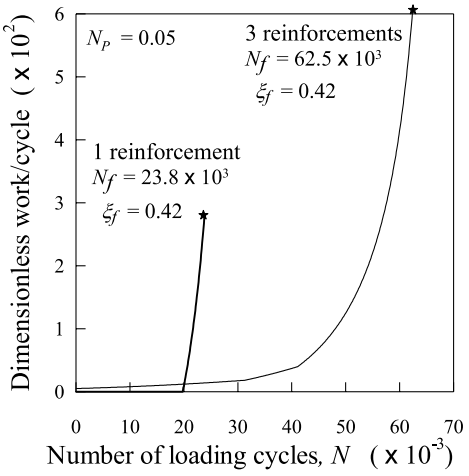

Fig. 10. Dimensionless dissipated energy (work/cycle multiplied by $E/(K_{IC}b)^2$) per hysteretic loop vs number of loading cycles, for both a single-reinforcement and a three-reinforcement beam ($\widetilde{M}_{\min} = 0, \widetilde{M}_{\max} = 0.10, N_{\mathrm{P}} = 0.05$).

5. Conclusions

A theoretical model based on fracture mechanics concepts is herein proposed to analyse the hysteretic behaviour of a brittle-matrix composite beam subjected to cyclic bending. Accordingly, a cracked beam with an elastic matrix and reinforcements acting as rigid-perfectly plastic bridging elements has been examined. The simple assumptions of the model allow us to describe typical cyclic phenomena, including elastic shake-down and plastic shake-down, and to predict fatigue life.

The capabilities of the model are presented in terms of applied bending moment against beam cross-section rotation, by pointing out that the response of the composite beam is dependent on the so-called brittleness number. The influence of such a parameter on the elastic behaviour, elastic shake-down and

plastic shake-down has been discussed by analysing some numerical examples. Furthermore, the energy dissipation in the hysteretic loops of plastic shake-down is shown to be influenced by the number of reinforcement elements among which a certain reinforcement area is distributed, the values of the other parameters being the same. For instance, if three reinforcements are considered instead of a single reinforcement, the total dissipated energy along with the fatigue life significantly increase.

Acknowledgements

The authors gratefully acknowledge the research support for this work provided by the Italian Ministry for University and Technological and Scientific Research (MIUR).

Appendix A

Let us consider a general linear-elastic plane stress problem for a cracked body. The body contains a through-thickness crack of length a, and is subjected to n generalised point loads F_i, $i = 1, \ldots, n$. The generic point-load translation δ_i can be expressed by the following relationship:

$$\delta_i = \sum_{j=1}^{n} \lambda_{ij} F_j \tag{A.1}$$

where λ_{ij} are the localised compliances.

For an increment of the crack length $\mathrm{d}a$, a variation of the total potential energy $\mathrm{d}W$ of the body occurs. Applying the Clapeyron theorem, such a variation can be expressed as follows:

$$\mathrm{d}W = -\sum_{i=1}^{n} \sum_{j=1}^{n} \frac{1}{2} F_i F_j \, \mathrm{d}\lambda_{ij} \tag{A.2}$$

where $\mathrm{d}\lambda_{ij}$ are the increments of the localised compliances due to crack extension $\mathrm{d}a$. Also, according to the Irwin relationship, the variation of the total potential energy $\mathrm{d}W$ can be expressed by:

$$\mathrm{d}W = -\frac{(K_{I1} + \cdots + K_{In})^2}{E} t \, \mathrm{d}a = -\sum_{i=1}^{n} \sum_{j=1}^{n} \frac{K_{Ii} K_{Ij}}{E} t \, \mathrm{d}a \tag{A.3}$$

where the generic K_{Ii} is the stress intensity factor at the crack tip due to the generalised force F_i.

Integration of Eqs. (A.2) and (A.3) yields two expressions for the variation of the total potential energy due to the presence of the crack with length a:

$$W = -\sum_{i=1}^{n} \sum_{j=1}^{n} \frac{1}{2} F_i F_j \lambda_{ij} \tag{A.4}$$

$$W = -\sum_{i=1}^{n} \sum_{j=1}^{n} \int_0^a \frac{K_{Ii} K_{Ij}}{E} t \, \mathrm{d}a' \tag{A.5}$$

Juxtaposing Eqs. (A.4) and (A.5), the generic localised compliance λ_{ij} can be defined as:

$$\lambda_{ij} = \frac{2}{E} \int_0^a \frac{K_{Ii} K_{Ij}}{F_i F_j} t \, \mathrm{d}a' \tag{A.6}$$

For the beam element in Fig. 1, the localised compliances can be calculated from Eq. (A.6) by considering the stress intensity factors for the applied loads, namely for the bending moment M and the reinforcement

reactions F_i, $i = 1, \ldots, n$. The expressions here adopted for the stress intensity factors are taken from (Tada et al., 1985), i.e.

$$K_{IM} = \frac{M}{b^{1.5}t} Y_M(\xi) \tag{A.7}$$

$$K_{Ii} = \frac{F_i}{b^{0.5}t} Y_{\mathrm{F}}(\xi, \zeta_i) \tag{A.8}$$

where

$$Y_M(\xi) = \begin{cases} 6\left(1.99\xi^{0.5} - 2.47\xi^{1.5} + 12.97\xi^{2.5} - 23.17\xi^{3.5} + 24.8\xi^{4.5}\right) & \xi \leqslant 0.6 \\ \frac{3.99}{(1-\xi)^{1.5}} & \xi > 0.6 \end{cases} \tag{A.9}$$

and

$$\begin{aligned} Y_{\mathrm{F}}(\xi, \zeta_i) &= \frac{2}{\sqrt{\pi\xi}} \frac{1}{(1-\xi)^{1.5}\sqrt{1 - \left(\frac{\zeta_i}{\xi}\right)^2}} G(\xi, \zeta_i) \quad \text{for } \xi \geqslant \zeta_i \\ G(\xi, \zeta_i) &= g_1(\xi) + g_2(\xi)\frac{\zeta_i}{\xi} + g_3(\xi)\left(\frac{\zeta_i}{\xi}\right)^2 + g_4(\xi)\left(\frac{\zeta_i}{\xi}\right)^3 \\ g_1(\xi) &= 0.46 + 3.06\xi + 0.84(1-\xi)^5 + 0.66\xi^2(1-\xi)^2 \\ g_2(\xi) &= -3.52\xi^2 \\ g_3(\xi) &= 6.17 - 28.22\xi + 34.54\xi^2 - 14.39\xi^3 - (1-\xi)^{1.5} - 5.88(1-\xi)^5 - 2.64\xi^2(1-\xi)^2 \\ g_4(\xi) &= -6.63 + 25.16\xi - 31.04\xi^2 + 14.41\xi^3 + 2(1-\xi)^{1.5} + 5.04(1-\xi)^5 + 1.98\xi^2(1-\xi)^2 \end{aligned} \tag{A.10}$$

By inserting Eqs. (A.7)–(A.10) in Eq. (A.6), the localised compliances λ_{ij}, λ_{iM} and λ_{MM} can be obtained:

$$\lambda_{ij} = \lambda_{ji} = \frac{2}{tE} \int_{\max\{\zeta_i, \zeta_j\}}^{\xi} Y_{\mathrm{F}}\left(\xi', \zeta_i\right) Y_{\mathrm{F}}\left(\xi', \zeta_j\right) \mathrm{d}\xi' \tag{A.11}$$

$$\lambda_{iM} = \frac{2}{btE} \int_{\zeta_i}^{\xi} Y_{\mathrm{F}}\left(\xi', \zeta_i\right) Y_M(\xi') \, \mathrm{d}\xi' \tag{A.12}$$

$$\lambda_{MM} = \frac{2}{b^2tE} \int_0^{\xi} Y_M^2(\xi') \, \mathrm{d}\xi' \tag{A.13}$$

Details on how to overcome the singularities in the integrals (A.11) and (A.12) are given in (Carpinteri Al and Massabò, 1997).

References

Baluch, M.H., Qureshy, A.B., Azad, A.K., 1987. Fatigue crack propagation in plain concrete. In: Shah. S.P., Swartz, S.E. (Eds.), Proceedings of the SEM/RILEM International Conference on Fracture of Concrete and Rock, Houston, Texas, pp. 80–87.

Carpinteri Al, 1984. Stability of fracturing process in RC beams. Journal of Structural Engineering ASCE 110, 544–558.

Carpinteri Al, Carpinteri An, 1984. Hysteretic behavior of RC beams. Journal of Structural Engineering ASCE 110, 2073–2084.

Carpinteri Al, Massabò, R., 1996. Bridged versus cohesive crack in the flexural behaviour of brittle-matrix composites. International Journal of Fracture 81, 125–145.

Carpinteri Al, Massabò, R., 1997. Continuous vs discontinuous bridged-crack model for fiber-reinforced materials in flexure. International Journal of Solids and Structures 34, 2321–2338.

Carpinteri Al, Puzzi, S., 2003. Hysteretic flexural behaviour of brittle matrix fibrous composites: the case of two fibers. In: Proceedings of the 16th AIMETA Congress of Theoretical and Applied Mechanics, Ferrara, Italy.

Carpinteri An, 1991. Energy dissipation in R.C. beams under cyclic loadings. Engineering Fracture Mechanics 39, 177–184.

Carpinteri An, 1992. Reinforced concrete beam behavior under cyclic loadings. In: Carpinteri Al (Ed.), Applications of Fracture Mechanics to Reinforced Concrete. Elsevier Science Publishers, UK, pp. 547–578.

Chaboche, J.L., 1986. Time-dependent constitutive theories for cyclic plasticity. International Journal of Plasticity 2, 149–188.

Masing, G., 1926. Eigenspannungen und verfestigung beim Messing. In: Proceedings of the 2nd International Conference of Applied Mechanics, Zurich, pp. 332–335 (in German).

Matsumoto, T., Li, V.C., 1999. Fatigue life of fiber reinforced concrete with a fracture mechanics based model. Cement & Concrete Composites 21, 249–261.

Paris, P.C., Erdogan, F., 1963. A critical analysis of crack propagation laws. Journal of Basic Engineering 85, 528–534.

Tada, H., Paris, P.C., Irwin, G., 1985. The Stress Analysis of Cracks. Paris Productions Incorporated (and Del Research Corporation), St. Louis, Missouri.

Zhang, J., Stang, H., 1998. Fatigue performance in flexure of fiber reinforced concrete. ACI Materials Journal 95, 58–68.

Zhang, J., Stang, H., Li, V.C., 1999. Fatigue life prediction of fiber reinforced concrete under flexural load. International Journal of Fatigue 21, 1033–1049.